

Published in final edited form as:

*J Mol Biol.* 2008 February 15; 376(2): 541–553.

## Mechanism of T7 RNAP Pausing and Termination at the T7 Concatemer Junction: A Local Change in Transcription Bubble Structure Drives a Large Change in Transcription Complex Architecture

Dhananjaya Nayak, Sylvester Siller, Qing Guo, and Rui Sousa\*

From the Department of Biochemistry, University of Texas Health Science Center, 7703 Floyd Curl Drive, San Antonio, Texas 78229

### Summary

The T7RNA polymerase elongation complex (EC) pauses and is destabilized at a unique 8 nt sequence found at the junction of the head to tail concatemers of T7 genomic DNA generated during T7 DNA replication. The paused EC may recruit the T7 DNA processing machinery, which cleaves the concatemered DNA within this 8 nt concatemer junction (CJ). Pausing of the EC at the CJ involves structural changes in both the RNAP and transcription bubble. However, these structural changes have not been fully defined, nor is it understood how the CJ sequence itself causes the EC to change its structure, pause, and become less stable. Here we use solution and RNAP-tethered chemical nucleases to probe the CJ transcript and changes in the EC structure as the polymerase pauses and terminates at the CJ. Together with extensive mutational scanning of regions of the polymerase likely to be involved in recognition of the CJ, we are able to develop a description of the events that occur as the EC transcribes through the CJ and subsequently pauses. In this process a local change in the structure of the transcription bubble drives a large change in the architecture of the EC. This altered EC structure may then serve as the signal that recruits the processing machinery to the CJ.

### Keywords

RNA polymerase; T7 RNA polymerase; DNA melting; DNA bending; transcription elongation; transcription termination

### Introduction

The functions of transcribing RNA polymerases (RNAPs) are not limited to synthesis of RNA. DNA damage or particular template sequences can cause transcription complexes (TCs) to pause and change conformation. The modified TC can then act as a signal that recruits cellular machinery for specific purposes<sup>1; 2; 3; 4; 5; 6</sup>. An example of this is the RNAP encoded by the T7 bacteriophage. This polymerase not only transcribes the T7 phage genes, but is also

Address correspondence to: Rui Sousa, Dept. of Biochemistry, U. Of Texas Health Sci. Ctr., 7703 Floyd Curl Drive, San Antonio, TX 78229–3900, Tel. 210–567–8782; Fax: 210–567–8778; E-mail: sousa@biochem.uthscsa.edu.

**Publisher's Disclaimer:** This is a PDF file of an unedited manuscript that has been accepted for publication. As a service to our customers we are providing this early version of the manuscript. The manuscript will undergo copyediting, typesetting, and review of the resulting proof before it is published in its final citable form. Please note that during the production process errors may be discovered which could affect the content, and all legal disclaimers that apply to the journal pertain.

involved in the process by which the head to tail concatemers of T7 genomes generated during T7 DNA replication are cut into single genomes and packaged into phage. In vitro, processing of the concatemeric DNA requires transcription by T7 RNAP<sup>7</sup>. The T7 RNAP elongation complex (EC) pauses 7–8 b.p. downstream of the unique 8 base pair sequence (fig. 1a) found between the concatemerized genomes<sup>8; 9; 10</sup>. This appears to be a critical step in T7 DNA processing as mutant RNAPs that fail to pause at the concatemer junction (CJ) sequence cannot support phage replication<sup>8; 9; 10</sup>. Both the left and right ends of mature T7 DNA are generated from cleavage within the CJ<sup>11</sup>, suggesting that the paused T7RNAP EC is involved in recruiting the processing machinery to the CJ.

The CJ not only causes the EC to pause, it also destabilizes it. *In vitro*, only ~1/4th of T7RNAP ECs terminate at the template sequence containing the CJ from the T7 genome<sup>10</sup>. The function of the 8 nt CJ sequence is maintained irrespective of the sequence context in which it is placed, but the 8 nts immediately downstream of the CJ modulate the fraction of paused ECs that terminate, with increases in the AT content of this sequence leading to increases in termination and shorter pause half-lives<sup>8; 9; 12; 13</sup>. T7 lysozyme, a regulator of T7 transcription that inhibits transcription of T7 genes encoding proteins involved in T7 DNA replication<sup>14</sup>, also increases pausing and termination at the CJ<sup>8</sup>. Thus, through the action of T7 lysozyme, the switch in the T7 transcriptional program from genes required for DNA replication to genes required for formation of the phage particle may be coordinated with processing of the concatemeric T7 DNA. Pausing at the CJ leads to a drastic change in the structure of the EC<sup>15</sup>, including an apparent shortening of the transcription bubble from 8–10 b.p. to 4–5 b.p. due to reannealing of the upstream half of the bubble<sup>16</sup>. Further conformational changes in the RNAP are required for termination as engineering of conformationally restricting disulfide bonds between different polymerase subdomains can block termination, but not pausing<sup>13; 15</sup>.

Proper RNA displacement appears to be critical for CJ function as template structures that cause formation of extended RNA:DNA hybrids also fail to efficiently pause and terminate at the CJ<sup>8; 12</sup>. This raises the possibility that an altered RNA structure is involved in CJ pausing and termination. However, unlike those sequences that encode RNAs with a strong potential for hairpin formation and that mediate pausing and termination for both cellular and phage RNAPs<sup>17; 18; 19</sup>, the CJ sequence exhibits no similarly unambiguous potential for formation of a hairpin or alternate base-paired structure. It is therefore unclear how the CJ is recognized, nor have the structural changes undergone by the EC and the mechanism by which these changes cause pausing and EC destabilization been defined.

To address these questions we have used solution and polymerase-tethered chemical nucleases to probe the CJ transcript and structural changes in the EC during pausing and termination at the CJ, and mutational scanning of the RNAP to identify residues involved in pausing and termination. Our results suggest a process in which formation of an alternate structure in the RNA facilitates displacement of the RNA:DNA hybrid and collapse of the transcription bubble. This, in turn, leads to a formation of a transcription complex with a drastically altered architecture that may then act as a signal to recruit the T7 DNA processing machinery to the CJ.

## Results

### The EC becomes unstable once it transcribes 3 nucleotides past the CJ

A recent study of T7 RNAP pausing and termination at a CJ element concluded that the EC becomes unstable as soon as it begins to transcribe the CJ sequence, at a point 14–15 nts upstream of the major sites of pausing and termination<sup>20</sup>. To evaluate this unexpected result we prepared T7RNAP ECs halted by 3'-dNMP incorporation at different positions on a

synthetic 66 nt T7 promoter template that encodes a 49 nt runoff transcript and that contains the 8 nt CJ sequence and an AT-rich downstream element to ensure high levels of termination (fig. 1A; referred to here as *HTSCJ66*). These reactions were then subject to ultrafiltration to separate transcripts that had been freed into solution (fig. 1A: “F”) from those that were still retained in transcription complexes (“R”). Runoff transcripts (“R.O.”) are released into solution as are the short (<6 nt) abortive transcript (figs. 1A, 1B). However, transcripts from 11 to 24 nts in length are effectively retained with the EC, with typically less than 10% being released (fig. 1B). ECs with transcripts 25 and 27–29 nts in length exhibit a modest decrease in stability, as assessed from the appearance of 20–30% of these transcripts in solution, however the first large decrease in complex stability is seen upon extension of the transcript to 26 nts (70% released). Ninety percent of the 30/31 nt transcripts (corresponding to the major pause/termination site on this template) are released (fig. 1B). Thus, unlike what was previously reported<sup>20</sup>, we do not observe the EC becoming significantly destabilized until it has transcribed 3 nts past the end of the CJ. To corroborate this result we compared termination in the presence and absence of T7 lysozyme, which enhances CJ pausing and termination<sup>8</sup>. In the absence of lysozyme, termination occurs predominately at +30/31, with a minor site at +26 (fig. 1C, lane 1). In the presence of lysozyme, the major sites of termination are shifted 2 nts upstream to +28 and +29, and +26 also becomes a major termination site, while +25 and +27 become minor sites (fig. 1C, lane 2). These patterns agree with the data from the ultrafiltration experiments that indicate that the EC begins to destabilize once it has transcribed 2 nts past the end of the CJ (at +25), with destabilization transiently increasing 3 nts past the CJ (at +26) and becoming maximal 7–8 nts past the end of this element.

### Identification of 2 classes of T7RNAP mutants that affect pausing and termination at the CJ

The results presented in fig. 1 indicate that the T7RNAP EC is destabilized when the center of the CJ is situated 6–11 nts upstream of the RNA 3'-end. This would place the CJ element where it could interact with regions on the upstream face of the RNAP (fig. 2a). In agreement with this, a chemical nuclease tethered to residue 385 on the upstream face of the thumb subdomain (fig. 2a) cleaves in the center of the CJ in the paused EC<sup>15</sup>. The T3 and Sp6 phage also exhibit a unique 8 nt sequence identical to the T7 CJ at a corresponding position in their genomes, suggesting that the respective RNAPs of all of these phages are capable of recognizing this sequence<sup>21</sup>, as has been shown *in vitro* for Sp6 RNAP<sup>22</sup>. We therefore identified residues on the polymerase upstream face that are identical in the T7, T3, and Sp6 RNAPs and introduced cysteines at these positions, reasoning that such residues are likely candidates for residues involved in CJ recognition. Following an initial characterization of the effects of these mutations on termination, additional charge altering (K to E and E to K) substitutions and multiple mutations were made to further define how the mutations were affecting recognition of the CJ. The positions of the mutated residues are illustrated in fig. 2a on the crystal structure of the T7RNAP EC<sup>23; 24</sup>. Several of the residues targeted for mutagenesis are located at the upstream edge of the transcription bubble and may be involved in defining the structure of the bubble (fig. 2b).

The effects of a subset of these mutations on termination on *HTSCJ66* are shown in fig. 3a and data for all the mutants is summarized in 3b. In these experiments reactions were incubated for 15–30 minutes, much longer than the duration of the pause, and ultrafiltration experiments (not shown) confirmed that transcripts shorter than the runoff correspond to termination products and not to paused ECs. Mutations in most of the targeted residues had no effects on CJ termination, even when multiple negative charges were introduced into the positively charged region that includes residues 407/412/332 that is expected to interact with the duplex DNA upstream of the transcription bubble<sup>25</sup>.

The mutants that did affect termination at the CJ element could be grouped into 2 classes based on their phenotypic effects, the character of the WT side-chain, and their location. One class corresponded to mutants in the (mostly aromatic) residues that define the upstream edge of the transcription bubble (Y178, W377, Y385, D388; fig. 2b). Mutants in these residues reduced termination at the CJ element (fig. 3b and 3a: lanes 7, 12–14). The other class included mutants of K206 and E207, where both increases and decreases in CJ termination are observed. Specifically, mutations that increase the net negative charge at these positions decrease CJ termination, while mutations that decrease the net negative charge increase termination. For example, K206C and K206E substitutions, which change the charge at this site by  $-1$  and  $-2$ , respectively reduce termination by approximately 2- and 3-fold (fig. 3b and 3a: lane 8). The E207C and E207K substitutions exhibit, respectively, 50% and 70% increases in the fraction of terminating complexes (3b and 3a: lane 9). Moreover, the conclusion that the net charge at 206/207, rather than specific amino acid identity, is the critical determinant of the amount of CJ termination is supported by the observation that mutations in one residue can suppress the effects of mutations in the other as is seen in the K206E/E207K and K206E/E207C mutants (fig. 3b).

In these experiments, we used a template in which the 8 nt sequence immediately downstream of the CJ element is more AT-rich than is the case for the CJ element in the T7 genome. This was done because it is otherwise difficult to detect changes in the small fraction of complexes that terminate at the genomic CJ. However, to confirm that the WT and mutant T7RNAPs behave similarly on the genomic element as on a CJ with an AT-rich downstream module, we also tested the termination efficiencies of these RNAPs on a CJ template with a downstream sequence identical to that found in the T7 genome (*Native CJ*). On this template the WT enzyme showed reduced termination relative to the more AT-rich template, but the effects of the Nicked or mutant enzymes on termination paralleled what was seen with the AT-rich template (fig. 3C: lanes 1–7). However these differences were often hard to detect because of the intrinsically low termination on the *Native CJ*. We therefore carried out a similar experiment with T7 lysozyme present. Under such conditions, the effects of mutations on the genomic CJ template are more clearly seen to directly parallel their effects on termination with the AT-rich template (fig. 3C: lanes 8–14). We conclude that the 8 nt CJ element functions similarly in both the T7 genomic and AT-rich context with the WT and mutant RNAPs, and that the 8 nts immediately downstream of the CJ modulate the amount of termination.

### Mutations in residues near the upstream edge of the transcription bubble disrupt RNA displacement

It has been reported that template structures that disrupt RNA displacement by T7 RNAP also reduce termination at the CJ<sup>8; 9; 10</sup>, suggesting that efficient RNA displacement is required for termination. We therefore characterized the RNA displacement activity of the mutations that affect CJ termination. Halted ECs were formed with these mutants and then treated with varying concentrations of hybrid specific RNase H or single-strand specific RNase T1 (fig. 4). If the enzymes exhibit effective RNA displacement then we observe that the RNA that has emerged from the EC is sensitive to RNase T1 and resistant to RNase H. Conversely, if RNA displacement is ineffective then the emerging RNA forms an extended hybrid that is T1 resistant but RNase H sensitive. The WT enzyme exhibits efficient RNA displacement and the emerging transcript is completely sensitive to RNase T1 (fig. 4, lanes 2–5) and resistant to RNase H (lanes 6–9). An RNAP that is proteolytically ‘nicked’ (the two fragments remain associated via non-covalent interactions) between aa 172 and 173 provides a positive control for an enzyme that is strongly deficient in both CJ termination and RNA displacement<sup>8; 26</sup>: the RNA in the nicked EC is highly resistant to T1 (lanes 11–14) but fully sensitive to RNase H. Mutations in residues 206/207, which also affect termination, were found to have RNA displacement activity like the WT enzyme (not shown). However, mutations in the aromatic

side-chains that define the upstream edge of the transcription bubble (fig. 2b), and that show reduced CJ termination (fig. 3), exhibit reduced RNA displacement activity manifest as levels of RNase T1 and H sensitivity (fig. 4, lanes 19–45) that are intermediate between those of the WT and Nicked enzymes. The reduced levels of CJ termination for these mutants therefore correlate with reduced RNA displacement.

### Encounter with the CJ leads to unbending of the upstream DNA

While mutation of residues at the upstream edge of the transcription bubble may affect pausing and termination at the CJ by altering transcription bubble structure, the effects of charge altering mutations at residues 206/207 suggest that these side-chains make electrostatic interactions with the upstream duplex DNA when the EC pauses or terminates at the CJ. This result is unexpected since the upstream DNA has been proposed to be sharply bent at the upstream edge of the transcription bubble and to interact with a positively charged region that includes residues 407/412<sup>25</sup> (fig. 2a). A possible explanation for this result is that during pausing or termination the upstream DNA moves away from residues 407/412 and towards 206/207. To test this we compared the cleavage patterns, in normal and CJ-paused ECs, of chemical nucleases tethered to cysteines introduced at 407 or 412, or at sites on the N-terminal domain (130, 239, 207), that could be informative of how the upstream DNA is bound in the EC. Though a previous study using tethered chemical nucleases revealed large structural changes in the EC upon pausing at the CJ<sup>15</sup>, that study utilized primarily nucleases attached to residues located downstream of the upstream edge of the transcription bubble and was not informative of the structural changes occurring upstream of the bubble.

ECs halted at +15, immediately upstream of the CJ, or +19, in the middle of the CJ, were formed by inclusion of 3'-dUTP or 3'-dCTP in transcription reactions with *HTSCJ66*. In the +15 halted EC, the nucleases tethered to residues 130, 239, or 207 give rise to a single Gaussian distribution of cleavages on the NT strand centered ~10 nts upstream of the RNA 3'-end (fig. 5a: lanes 2, 7, 22) while the nucleases tethered to 407 or 412 give rise to 2 sets of cuts centered ~15 and ~25 nts upstream of the RNA 3'-end, with the nuclease tethered to 412 exhibiting stronger cleavage at the more upstream site and the nuclease at 407 cutting more strongly at the more downstream site (fig. 5a: lanes 12, 17). In the EC halted at +19 the pattern of all the cleavages is the same as in the +15 EC, except that the cut sites are shifted downstream by ~4 nts (lanes 3, 8, 13, 18, 23). These cutting patterns are consistent with an EC structure in which the DNA is sharply bent at the upstream edge of the transcription bubble and then approaches residues 407/412 (fig. 5c: "Normal EC").

To characterize the cleavage pattern of complexes paused at the CJ we stopped ECs at +14 by omitting UTP and CTP from transcription reactions and then chased these complexes with the missing NTPs. Ten seconds after initiation of the chase, cleavage by the chemical nucleases was activated in a reaction sample by addition of ascorbate and hydrogen peroxide, revealing cleavage from ECs paused at +30/31 on the CJ (fig. 5a: lanes 4, 9, 14, 19, 24). That these cuts are due to paused ECs is confirmed by examining cleavage in a reaction sample taken 10 minutes after the chase (lanes 5, 10, 15, 20, 25), at which point the paused ECs have either terminated or read through the CJ (pause half life has been estimated at 20–30 sec.<sup>9; 15</sup>), and cleavage is expected to be greatly reduced. Unlike the simple translocation that relates the cleavage patterns of ECs halted at +19 vs. +15, the cuts originating from the EC paused at the CJ reveal a large structural change in the transcription complex. First, the cut sites do not move as far downstream as expected: if only simple translocation were occurring then complexes paused at +30/31 should cleave 11–12 nts downstream of those halted at +19. Second, the patterns of cutting change: nucleases at 130, 239, and 207 in the paused EC exhibit two centers of cleavage spaced ~11 nts apart and centered ~3 nts downstream and ~8 nts upstream of the single cleavage site seen in the +19 EC (compare lanes 3 and 4, 8 and 9, 23 and 24). Detection



of 2 centers of cleavage spaced ~11 nt apart is characteristic of the nuclease being opposite one face of a duplex so that each strand is alternately exposed and protected from the nuclease with a 10–11 nt periodicity. Finally, cleavage by the nucleases tethered to 407 or 412 in the paused ECs is undetectable. This is not due to abrogation of pausing or termination by the cysteines introduced at 407 and 412 since the K407C and K412C mutants terminate like the WT enzyme (fig. 3).

Instead, the absence of cleavage by the nucleases at 407/412 suggests that upstream DNA moves away from these residues in the paused complex. Moreover the changes in cutting patterns by the nucleases at 130, 239, and 207 suggest further that as the DNA swings away from residues 407/412, it swings towards residue 207 (fig. 5c: “Paused EC”). In particular, this is suggested by the increase in cleavage seen with the nuclease at 207 in the paused vs. normal EC: the total integrated intensity for the two cleavage sites in the paused complex is 2–3 fold greater than for the single site in the normal EC (compare lanes 22 or 23 with lane 24 in fig. 5a). For the nucleases at 239 and 130 the total cleavage intensity in the paused EC is comparable to that seen in the normal ECs (compare lanes 4 and 9 to 3 and 8, respectively), but it must be remembered that, 10 seconds after initiation of the chase, only ~50% of ECs are paused at the CJ (the remaining 50% have either read-through or terminated), so we would expect the total cleavage intensity by the 239 and 130 nucleases to decrease in the paused vs. normal ECs unless the upstream DNA moves closer to these residues (the increased cleavage intensity in the paused vs. normal EC with the 207 nuclease likely reflects both that the DNA has moved closer to this residue and that the E207C mutant increases the fraction of complexes that pause and terminate at the CJ (fig. 3)).

Movement of the DNA away from residues 407/412 and towards residue 207 would relax the bend at the upstream edge of the transcription bubble that is present in the normal EC. Since duplex DNA is relatively rigid, such unbending would be favored by the collapse of the upstream half of the transcription bubble that occurs once the EC transcribes 3 nts past the CJ<sup>16; 20</sup>. This coupled unbending and partial bubble collapse would partially account for the observation that the cut sites of nucleases tethered to the upstream face of the RNAP N-terminal domain are farther upstream (relative to the RNA 3'-end) in the paused EC than in a normal EC (fig. 5c: “Bubble Collapsed EC”). The shifts in these cleavage sites could be fully accounted for if, following the initial bubble collapse and change in EC architecture, the translocation of the polymerase were inhibited by the new interactions made with the upstream DNA. To ask whether such inhibition of translocation occurs, as well as to determine at what point the structural change in the EC happens, we used the tethered chemical nucleases to probe EC structure on a template (+28 A CJ) that allowed us to halt the complex 5 nts past the CJ (at +28), corresponding to a point subsequent to bubble collapse but prior to the major pause/termination site (fig. 5b). We found that the cleavage patterns in the ECs halted at +28 were similar and identically positioned to those of complexes paused at +30/31, and unlike those of complexes halted at +15 or +19 (compare figs. 5a and 5b). This indicates that the change in the EC structure occurs before it reaches the pause/termination site and most likely coincides with the collapse of the transcription bubble. It further suggests that, once this change occurs, the RNAP N-terminal domain to which the chemical nucleases at 130/207/239 are tethered no longer translocates along the DNA (fig. 5c: “Paused EC”). Though it is possible that the introduced mutations or the conjugates themselves are affecting EC structure, particularly for E207C which affects % termination, the observation that the results with all 5 of these conjugates (at aa 130/207/239/407/412) are consistent with the change in EC structure modeled in figs. 5a-c implies that these structural changes are intrinsic to the process of pausing at the CJ, and are not a consequence of the introduction of a particular mutation.

## The CJ RNA may form an alternate structure that competes with the RNA:DNA hybrid

The central element of the mechanism of pausing and termination at the CJ may be the collapse of the upstream half of the transcription bubble. This single change could explain: 1. the destabilization of the complex due to the shortening of the hybrid length, 2. the unbending of the upstream DNA due to reannealing of the duplex at the bend, and 3. the pausing of the EC 4–5 nts downstream of the point of bubble collapse due to the establishment of a new set of upstream DNA:RNAP interactions that restrain EC translocation (fig. 5).

What features of the CJ sequence lead to the collapse of the bubble? One possibility is the formation of an alternate structure in the RNA that reduces the net free energy of RNA displacement, allowing the NT strand to reanneal with the T strand. Though the CJ sequence exhibits no alternate base-paired structure that could compete with hybrid formation, it does display a sequence identical to the 5 nt AUCUG element of the HIV Tar RNA hairpin bulge (fig. 6A)<sup>27</sup>. The Tar RNA bulge structure is constrained by the base pairs that flank the central unpaired UCU but the sequence of this element is also critical for assumption of its characteristic structure, which is stabilized by binding of arginine<sup>28</sup> or divalent metal ions such as Mg<sup>++</sup>, Ca<sup>++</sup>, and Pb<sup>++</sup><sup>29; 30</sup>.

Bound lead ions can cleave the RNA backbone and 1 mM Pb<sup>++</sup> cleaves strongly at the central C of the Tar AUCUG sequence<sup>30</sup>. To determine if the CJ RNA could form a structure that would be similarly bound and cleaved by Pb<sup>++</sup> we incubated 5'-end labeled CJ transcripts with 1 mM Pb<sup>++</sup> and observed strong cleavage at the central C of the CJ element against a weaker background of Pb<sup>++</sup> cutting at all sites (fig. 6B, lanes 1–3). This background cleavage provides an internal control and measure of the specificity of cutting at the central C of the CJ. In lane 2 of the experiment shown in fig. 6B, ~60% of the 30/31 nt transcripts have been cut by Pb<sup>++</sup> as compared to the reaction in lane 1. Cutting at the central C of the CJ sequence accounts for ~25% of the cleaved products, indicating a ~10-fold higher cleavage at this C than the average at other sites on the transcript (a similar degree of enhancement is obtained if we calculate the % radioactivity in individual cleavage products after first subtracting the untreated background (solid trace next to fig. 6B, lane 3) from the Pb<sup>++</sup> treated reaction (dotted trace)). Transcripts from a template containing a single A->U change in the first A of the CJ RNA (*Mut CJ*) were similarly probed with lead. The A->U change in the CJ reduces pausing and termination by more than 60%, and eliminates the enhanced cleavage at the central C of the WT CJ transcript (fig. 6C, lanes 4–6).

The Pb<sup>++</sup> reactivity indicates that the portion of the CJ transcript that is displaced from the DNA during pausing/termination can form a metal binding site. RNA folding is stabilized by interactions with metal ions and arginine side-chains<sup>31; 32</sup>. Metal ions and arginine could therefore be expected to stabilize a folded structure in the displaced CJ RNA and to enhance pausing/termination. We therefore tested the effects of varying MgCl<sub>2</sub> and arginine concentrations on termination at the CJ. As controls we tested NaCl and lysine, which has been reported to bind and stabilize the Tar bulge, but to a lesser extent than arginine<sup>28</sup>. Concentrations of lysine and NaCl in excess of 50 mM caused modest increases in pausing/termination and at higher concentrations inhibited transcription (fig. 7a, lanes 1–10). At equal concentrations arginine increased termination to a markedly greater extent than either NaCl or lysine, while Mg<sup>++</sup> caused similar increases in termination at concentrations of 10 mM (fig. 7b and 7a, lanes 11–24).

## Discussion

The results presented here, together with previous studies, allow us to develop the following model for the process of pausing and termination at the T7 concatemer junction:

1. As the EC transcribes through the end of the CJ it maintains a constant structure, with an 8–10 nt transcription bubble and a bend at the upstream edge of the bubble that directs the upstream duplex DNA towards residues 407/412 (fig. 5c: “Normal EC”). We base this conclusion on the following: i. the cleavage patterns of polymerase-tethered chemical nucleases are identical for an EC halted 4 nts into the CJ (at +19 on the template used here) and for an EC halted 1 nt before the CJ (at +15; figs. 5a,b); ii.  $\text{KMnO}_4$  probing reveals the bubble to be 8–10 nts in size for ECs halted 2 nts before the end of the CJ element, at the very end of the CJ, or 1 or 2 nts past the CJ<sup>20</sup>.
2. When the EC transcribes 3 nts past the end of the CJ, the upstream half of the transcription bubble collapses, leaving behind a 3 b.p. RNA:DNA hybrid. The reannealing of the T and NT strands in the upstream region of the bubble leads to unbending of the upstream DNA so that it moves away from residues 407/412 and towards 207 (fig. 5c: “Bubble Collapsed EC”). We base this conclusion on the following observations: i.  $\text{KMnO}_4$  probing reveals collapse of the upstream region of the bubble once the EC transcribes 3 nts past the CJ<sup>20</sup>; ii. tethered chemical nuclease cleavage patterns are consistent with the postulated unbending of the upstream DNA in ECs stopped 5 (at +28) or 7–8 (at +30/31) nts past end of the CJ (fig. 5a, b); iii. the EC becomes especially unstable *precisely* 3 nts past the end of the CJ (at +26), as can be seen both in experiments where dissociation of ECs halted at different positions on the template is measured (figs. 1a, b) or when transcription reactions are carried out in the presence of T7 lysozyme which enhances termination by further destabilizing the EC (fig. 1c; the peculiar increase in termination 3 nts past the CJ has also been noted previously and this position corresponds to what has been dubbed the minor (T1) termination site<sup>12</sup>). Our conclusion that the EC becomes unstable when it transcribes 3 nts past the CJ disagrees with a recent study that concluded that it begins to destabilize as soon as it begins to transcribe the CJ<sup>20</sup>. We cannot explain these differences but we note that our own experiments and those probing bubble size indicate that the EC structure does not change until the polymerase has transcribed past the CJ, and that an experiment measuring Sp6 RNAP EC stability on a CJ template obtained results identical to those we present in fig. 1, namely a spike in EC instability 3 nts past the CJ before it becomes maximally unstable 7–8 nts downstream of the CJ at the major pause/termination sites (see fig. 8 of ref. <sup>22</sup>).
3. Following bubble collapse and DNA unbending at CJ+3, transcription continues with the EC becoming *more* stable due to the extension in the size of the RNA:DNA hybrid. However, the new interaction with the upstream DNA, unlike the interaction present in an EC of normal structure, restrains the translocation of the N-terminal domain. Continued transcription is accommodated by some combination of DNA scrunching and/or limited conformational adjustments in the RNAP (possibly movements of the N-terminal domain analogous to those suggested to explain transcript extension during initiation<sup>33</sup>) until such adjustments reach a limit 4–5 nts past the initial point of bubble collapse and the polymerase must pause. At this point, however, the extension of the transcript means that a normal bubble and hybrid size has been recovered (fig. 5c: “Paused EC”) and the EC may either release the upstream interaction, recover its normal structure and continue transcription, or the EC instability induced by the scrunching and/or conformational accommodations may result in EC dissociation and termination, with the latter being favored if the hybrid is AU-rich. We base these conclusions on the following observations: i.  $\text{KMnO}_4$  probing reveals that, following bubble collapse at CJ+3, the bubble grows in size as the RNA is subsequently extended<sup>16; 20</sup>, ii. EC dissociation and termination experiments show that the EC becomes more stable as the RNA is extended beyond CJ+3 (fig. 1), iii. nucleases tethered to the RNAP N-terminal domain cut the DNA at



the same positions when the EC is halted at CJ+5 or when it is paused at CJ+7/8 (figs. 5a, b).

That the RNAP conformational changes accompanying pausing are likely to be limited is suggested by the following: i. it is possible to largely account for the changes in tethered chemical nuclease cutting patterns in the paused vs. normal EC in terms of changes in nucleic acid architecture without invoking major RNAP conformational change, and ii. the introduction of disulfide cross-links into the RNAP that restrict conformational changes and prevent the isomerization of the RNAP from an EC to an IC conformation block termination, *but not pausing*, at the CJ<sup>13; 15</sup>. Major conformational changes therefore appear to be required only to allow the polymerase to release the transcript and template, consistent with observations that the free RNAP conformation is similar to that seen in the IC<sup>34; 35; 36</sup>.

In this process the crucial event is the collapse of the transcription bubble, which then leads to DNA unbending and establishment of the translocation restraining interaction with upstream DNA. It is not yet clear how the CJ sequence induces RNA displacement and bubble collapse but for the following reasons we think this is unlikely to involve a direct readout of the CJ sequence by RNAP side-chains: i. the KII, Sp6, T7, and T3 phage all display a sequence identical to the 8 nt CJ element at corresponding positions in their genomes, and the Sp6 and T7 RNAPs have been shown to pause and terminate at this element in an identical manner<sup>12; 22</sup>. Sp6 and T7 RNAPs are highly divergent, with only ~20% sequence identity in the upstream (N-terminal) regions that would be positioned to contact the CJ. We are unaware of any family of proteins that are so divergent and yet recognize the same DNA sequence through direct base read-out. ii. We carried out extensive mutational scanning of residues conserved in the Sp6, T7, and T3 RNAPs that would be positioned to contact the CJ during pausing/termination (fig. 2). We identified mutations that appeared to decrease termination by disrupting proper RNA displacement (figs. 2-4), and mutations that increase or decrease termination by either increasing or decreasing positive charge at position 206/207 (fig. 3). However, this mutational scan did not identify any residues whose mutant phenotypes indicated involvement in direct base readout of the CJ sequence.

Though such negative results cannot be conclusive, the alternative model that pausing at the CJ involves structural changes in the nucleic acids that alter the balance between RNA:DNA hybrid maintenance and DNA reannealing is well-supported. This evidence includes not only the direct evidence for such structural changes mentioned above and the observation that RNAP mutations that induce extended hybrids reduce termination at the CJ, but also observations that template modifications that reduce the driving force for DNA reannealing to favor formation of extended RNA:DNA hybrids (heteroduplexes, gapped NT strands, supercoiling, nucleotides that weaken T:NT strand pairing) also result in reduced pausing and termination at the CJ<sup>12; 37</sup>. One mechanism to alter the balance between RNA:DNA vs. DNA:DNA base pairing to favor transcription bubble collapse would be formation of an unpaired structure in the CJ transcript that reduces the free energy of RNA:DNA hybrid displacement. The detection of sequence identity between the CJ and the metal binding site of the Tar bulge (fig. 6a) and of CJ reactivity with Pb<sup>++</sup> (fig. 6b) similar to that seen with the Tar RNA<sup>30</sup> indicate that the CJ RNA can form a metal ion binding site. The observation that Mg<sup>++</sup> and arginine, which both stabilize RNA folding<sup>28; 31; 32</sup>, enhance termination at the CJ (fig. 7) is also consistent with the idea that pausing and termination at this element involve formation of an unpaired RNA structure that facilitates RNA:DNA hybrid displacement. Achieving a more detailed description of this alternate RNA structure will require higher resolution structural studies of ECs halted at the CJ. The observation that ECs halted 4–6 nts beyond the CJ have undergone bubble collapse<sup>20</sup> and a change in EC architecture (fig. 5), but are almost as stable as normal ECs (fig. 1), defines conditions under which stable ‘CJ-ECs’ may be prepared for such structural studies.

Ultimately, the biological function of pausing at the CJ appears to be to recruit the machinery required for processing of T7 DNA<sup>7, 11</sup>. We suggest that this processing machinery recognizes the drastically altered EC architecture that is induced by collapse of the transcription bubble. Such a mechanism would provide specificity in the processing reaction by preventing this machinery from being recruited to normal ECs that are either actively elongating or that have paused anywhere other than the unique 8 nt CJ element found in the genomes of T7 and related phage.

## Methods and Materials

### RNAP preparation

WT and mutant RNAPs were prepared as described<sup>25</sup>. Proteolytically nicked RNAP was prepared by incubating purified T7RNAP with whole *Escherichia coli* cells (strain HMS174) as described<sup>38</sup>.

### Template preparation

A set of 66 nt oligonucleotides having the following non-template sequences and their complementary template strands were synthesized and PAGE purified by Operon Biotechnologies:

	-17	+1	+15	+30	+45
HTSCG66:	5'-TAATACGACTCAC	<b>TATA</b> GGGAGAGGAAGAGATT	<u>TATCTGTTTCTTG</u>	<u>CCAAGTGAGTGGT</u>	AGATCGA-3'
Native CJ:				AGAGTGTC	
+28A CJ:				A	
Mut CJ:			T		

In each case the sequence from -17 to +5 corresponds to the T7 promoter consensus. The 8 nt (TATCTGTT) conserved CJ sequence and major pause/termination sites at +30/31 are underlined. Duplex templates were prepared by mixing equimolar amounts of T and NT-oligonucleotides in 10 mM Tris-HCl; pH 8.0, 40 mM NaCl, 1mM EDTA, heated to 90°C for 10 min followed by slow cooling to room temperature. Transcription reactions and DNA cleavage by Fe-BABE conjugated RNAPs were carried out as described<sup>15</sup>. In some transcription reactions NaCl, lysine, MgCl<sub>2</sub>, or arginine were added to the reaction buffer at concentrations specified in individual figures.

### Effect of T7 lysozyme on termination

ECs halted at +14 were formed on *HTSCJ66* or the *Native CJ* templates in transcription reactions with only GTP and ATP added (0.5 mM). Reactions were split in 2 and a 10-fold excess of T7 lysozyme (relative to RNAP) was added to one sample, following which reactions were chased with complete NTP mixes for 15 min at room temperature.

### RNA displacement as assessed by RNaseH and RNaseT1 sensitivity

ECs halted at +15 (EC15) were formed at room temperature in transcription buffer with *HTSCJ66* at 0.1 μM and RNAP at 0.3 μM in the presence of GTP, ATP and 3'-dUTP (0.5 mM). Reactions were then treated with either RNaseH or RNaseT1 at 0.25, 0.5, 1.0 and 2.0 U/μl for 15 min at 37° C. Reaction was stopped, resolved and analyzed as described for the transcription reactions.

### Pb<sup>2+</sup> induced RNA phosphodiester bond cleavage

Run off transcription reactions were carried out in transcription buffer containing *HTSCJ66* or *Mut CJ* templates at 0.1 μM and RNAP at 0.6 μM and NTPs at 0.5 mM. Transcripts were labeled at their 5' end by incorporation of 1% (v/v) [ $\gamma$ <sup>32</sup>P] GTP (6000 ci/mmol, Perkin Elmer)

into the reaction mixture. Released transcripts were separated from RNAP by passing through a centricon ultrafiltration unit (Amicon) of 100 kD MW cutoff. Transcripts were incubated with or without 1 mM Pb(OAc)<sub>2</sub> in 10 mM Tris-HCl; pH 7.2, 40 mM NaCl for 0.5–2 hr at 37° C as indicated in individual figure legends. Reactions were stopped, resolved and analyzed as mentioned previously.

#### Acknowledgments

Supports by NIH GM52522 and Welch Grant AQ-1486 (to R.S.). We thank Dr. William T. McAllister for first pointing out to us the similarity between the CJ sequence and the Tar-RNA hairpin bulge.

#### Abbreviations used

RNAP, RNA polymerase; nt, nucleotide or nucleotides; T-strand, template strand; NT-strand, Non-template strand; IC, Initiation complex; EC, Elongation complex; Fe-BABE, iron (S)-1-(p-bromoacetamidobenzyl)ethylenediamine-tetraacetate.

#### References

1. Deaconescu AM, Chambers AL, Smith AJ, Nickels BE, Hochschild A, Savery NJ, Darst SA. Structural basis for bacterial transcription-coupled DNA repair. *Cell* 2006;124:507–20. [PubMed: 16469698]
2. Laine JP, Egly JM. Initiation of DNA repair mediated by a stalled RNA polymerase II. *Embo J* 2006;25:387–97. [PubMed: 16407975]
3. Laine JP, Egly JM. When transcription and repair meet: a complex system. *Trends Genet* 2006;22:430–6. [PubMed: 16797777]
4. Fujita T, Ryser S, Tortola S, Piuze I, Schlegel W. Gene-specific recruitment of positive and negative elongation factors during stimulated transcription of the MKP-1 gene in neuroendocrine cells. *Nucleic Acids Res* 2007;35:1007–17. [PubMed: 17259211]
5. Eissenberg JC, Shilatifard A. Leaving a mark: the many footprints of the elongating RNA polymerase II. *Curr Opin Genet Dev* 2006;16:184–90. [PubMed: 16503129]
6. Pavri R, Zhu B, Li G, Trojer P, Mandal S, Shilatifard A, Reinberg D. Histone H2B monoubiquitination functions cooperatively with FACT to regulate elongation by RNA polymerase II. *Cell* 2006;125:703–17. [PubMed: 16713563]
7. Hashimoto C, Fujisawa H. Transcription dependence of DNA packaging of bacteriophages T3 and T7. *Virology* 1992;191:246–50. [PubMed: 1413505]
8. Lyakhov DL, He B, Zhang X, Studier FW, Dunn JJ, McAllister WT. Mutant bacteriophage T7 RNA polymerases with altered termination properties. *J Mol Biol* 1997;269:28–40. [PubMed: 9192998]
9. Lyakhov DL, He B, Zhang X, Studier FW, Dunn JJ, McAllister WT. Pausing and termination by bacteriophage T7 RNA polymerase. *J Mol Biol* 1998;280:201–13. [PubMed: 9654445]
10. Zhang X, Studier FW. Isolation of transcriptionally active mutants of T7 RNA polymerase that do not support phage growth. *J Mol Biol* 1995;250:156–68. [PubMed: 7608967]
11. Chung YB, Hinkle DC. Bacteriophage T7 DNA packaging. I. Plasmids containing a T7 replication origin and the T7 concatamer junction are packaged into transducing particles during phage infection. *J Mol Biol* 1990;216:911–26. [PubMed: 2266562]
12. He B, Kukarin A, Temiakov D, Chin-Bow ST, Lyakhov DL, Rong M, Durbin RK, McAllister WT. Characterization of an unusual, sequence-specific termination signal for T7 RNA polymerase. *J Biol Chem* 1998;273:18802–11. [PubMed: 9668054]
13. Ma K, Temiakov D, Anikin M, McAllister WT. Probing conformational changes in T7 RNA polymerase during initiation and termination by using engineered disulfide linkages. *Proc Natl Acad Sci U S A* 2005;102:17612–7. [PubMed: 16301518]
14. Moffatt BA, Studier FW. T7 lysozyme inhibits transcription by T7 RNA polymerase. *Cell* 1987;49:221–7. [PubMed: 3568126]
15. Mukherjee S, Briebe LG, Sousa R. Discontinuous Movements and Conformational Isomerizations During Pausing and Termination by T7 RNA Polymerase. *Embo J* 2003;22:6483–93. [PubMed: 14657021]

16. Song H, Kang C. Sequence-specific termination by T7 RNA polymerase requires formation of paused conformation prior to the point of RNA release. *Genes Cells* 2001;6:291–301. [PubMed: 11318872]
17. Macdonald LE, Durbin RK, Dunn JJ, McAllister WT. Characterization of two types of termination signal for bacteriophage T7 RNA polymerase. *J Mol Biol* 1994;238:145–58. [PubMed: 8158645]
18. Platt, T. RNA Structure and Function.. In: Simon, R.; Gunberg-Manago, M., editors. *RNA Structure and Function*. Cold Spring Harbor Laboratory; Cold Spring Harbor, NY: 1996. p. 541-547.
19. Chan, C.; Landick, R. Transcription: Mechanisms and Regulation.. In: Conaway, R.; Conaway, JW., editors. *Transcription: Mechanisms and Regulation*. Raven Press; New York: 1994. p. 297-321.
20. Sohn Y, Kang C. Sequential multiple functions of the conserved sequence in sequence-specific termination by T7 RNA polymerase. *Proc Natl Acad Sci U S A* 2005;102:75–80. [PubMed: 15615852]
21. Scholl D, Kieleczawa J, Kemp P, Rush J, Richardson CC, Merrill C, Adhya S, Molineux JJ. Genomic analysis of bacteriophages SP6 and K1–5, an estranged subgroup of the T7 supergroup. *J Mol Biol* 2004;335:1151–71. [PubMed: 14729334]
22. Kwon YS, Kang C. Bipartite modular structure of intrinsic, RNA hairpin-independent termination signal for phage RNA polymerases. *J Biol Chem* 1999;274:29149–55. [PubMed: 10506170]
23. Tahirov TH, Temiakov D, Anikin M, Patlan V, McAllister WT, Vassilyev DG, Yokoyama S. Structure of a T7 RNA polymerase elongation complex at 2.9 Å resolution. *Nature* 2002;420:43–50. [PubMed: 12422209]
24. Yin YW, Steitz TA. Structural basis for the transition from initiation to elongation transcription in T7 RNA polymerase. *Science* 2002;298:1387–95. [PubMed: 12242451]
25. Nayak D, Guo Q, Sousa R. Functional architecture of T7 RNA polymerase transcription complexes. *J Mol Biol* 2007;371:490–500. [PubMed: 17580086]
26. Gopal V, Brieba LG, Guajardo R, McAllister WT, Sousa R. Characterization of structural features important for T7 RNAP elongation complex stability reveals competing complex conformations and a role for the non-template strand in RNA displacement. *J Mol Biol* 1999;290:411–31. [PubMed: 10390341]
27. Weeks KM, Ampe C, Schultz SC, Steitz TA, Crothers DM. Fragments of the HIV-1 Tat protein specifically bind TAR RNA. *Science* 1990;249:1281–5. [PubMed: 2205002]
28. Tao J, Frankel AD. Specific binding of arginine to TAR RNA. *Proc Natl Acad Sci U S A* 1992;89:2723–6. [PubMed: 1557378]
29. Ippolito JA, Steitz TA. A 1.3-Å resolution crystal structure of the HIV-1 trans-activation response region RNA stem reveals a metal ion-dependent bulge conformation. *Proc Natl Acad Sci U S A* 1998;95:9819–24. [PubMed: 9707559]
30. Olejniczak M, Gdaniec Z, Fischer A, Grabarkiewicz T, Bielecki L, Adamiak RW. The bulge region of HIV-1 TAR RNA binds metal ions in solution. *Nucleic Acids Res* 2002;30:4241–9. [PubMed: 12364603]
31. Tinoco I, Jr. Bustamante C. How RNA folds. *J Mol Biol* 1999;293:271–81. [PubMed: 10550208]
32. Weiss MA, Narayana N. RNA recognition by arginine-rich peptide motifs. *Biopolymers* 1998;48:167–80. [PubMed: 10333744]
33. Turingan RS, Theis K, Martin CT. Twisted or shifted? Fluorescence measurements of late intermediates in transcription initiation by T7 RNA polymerase. *Biochemistry* 2007;46:6165–8. [PubMed: 17472344]
34. Sousa R, Chung YJ, Rose JP, Wang BC. Crystal structure of bacteriophage T7 RNA polymerase at 3.3 Å resolution. *Nature* 1993;364:593–9. [PubMed: 7688864]
35. Cheetham GM, Steitz TA. Structure of a transcribing T7 RNA polymerase initiation complex. *Science* 1999;286:2305–9. [PubMed: 10600732]
36. Cheetham GM, Jeruzalmi D, Steitz TA. Structural basis for initiation of transcription from an RNA polymerase-promoter complex. *Nature* 1999;399:80–3. [PubMed: 10331394]
37. Hartvig L, Christiansen J. Intrinsic termination of T7 RNA polymerase mediated by either RNA or DNA. *Embo J* 1996;15:4767–74. [PubMed: 8887568]
38. Muller DK, Martin CT, Coleman JE. Processivity of proteolytically modified forms of T7 RNA polymerase. *Biochemistry* 1988;27:5763–71. [PubMed: 2460133]

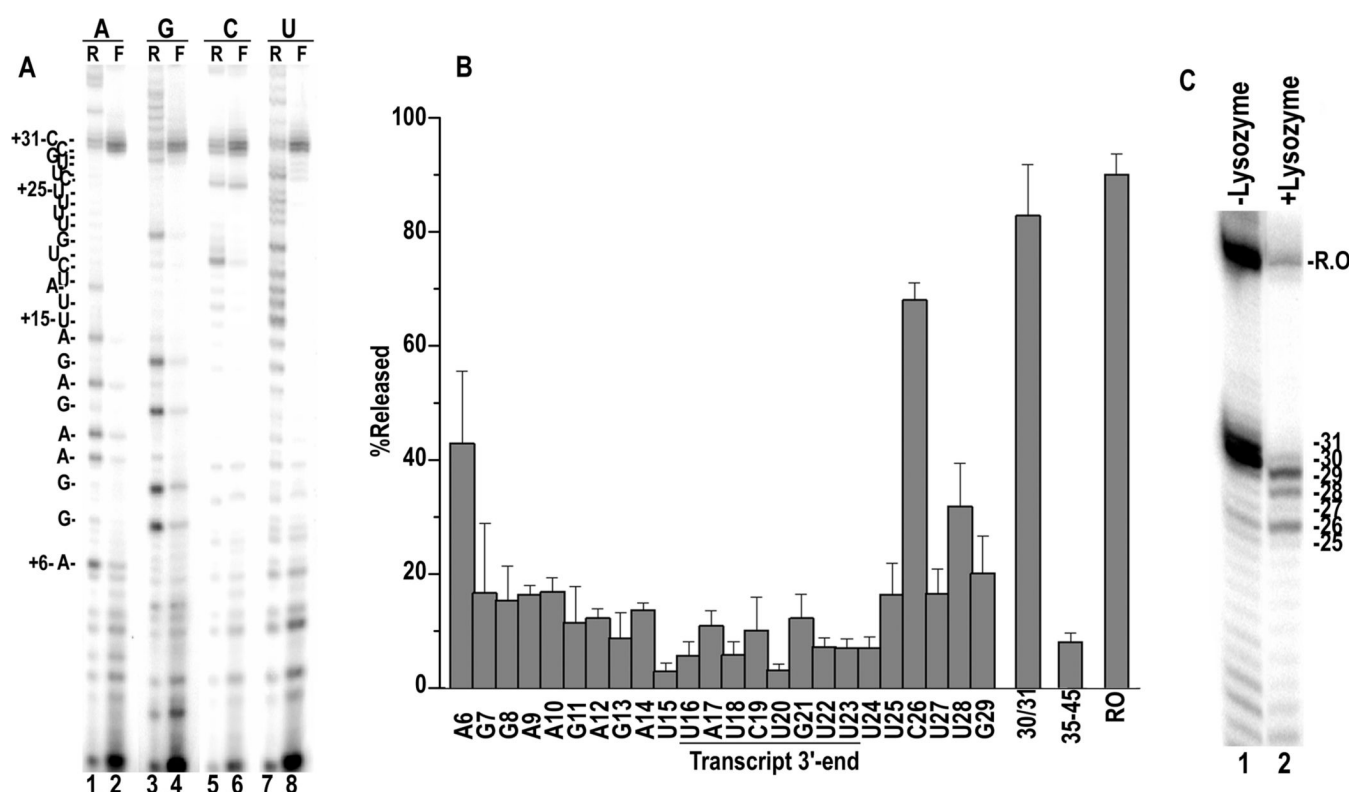


**Figure 1. The EC is destabilized 2–8 nts downstream of the CJ**

A: Denaturing PAGE of transcription reactions run on a synthetic template (*HTSCJ66*) with a –17 to +5 sequence matching the class I T7 promoter and the +6 to +31 sequence as shown. Reactions were spiked with 0.05 mM 3'-dATP (lanes 1, 2), 3'-dGTP (lanes 3, 4), 3'-dCTP (lanes 5, 6), or 3'-dUTP (lanes 7, 8) to form halted ECs, then filtered through membranes with 100kD cutoff to separate transcripts retained in the halted ECs ("R"; odd-numbered lanes) from those released into solution ("F"; even-numbered lanes). B: Plot of % transcripts released in experiments like those shown in A (error bars give ranges for n=3). C: Termination patterns in transcription reactions run on the template used in A in either the absence (lane 1), or presence (lane 2) of 10-fold excess of T7 lysozyme.



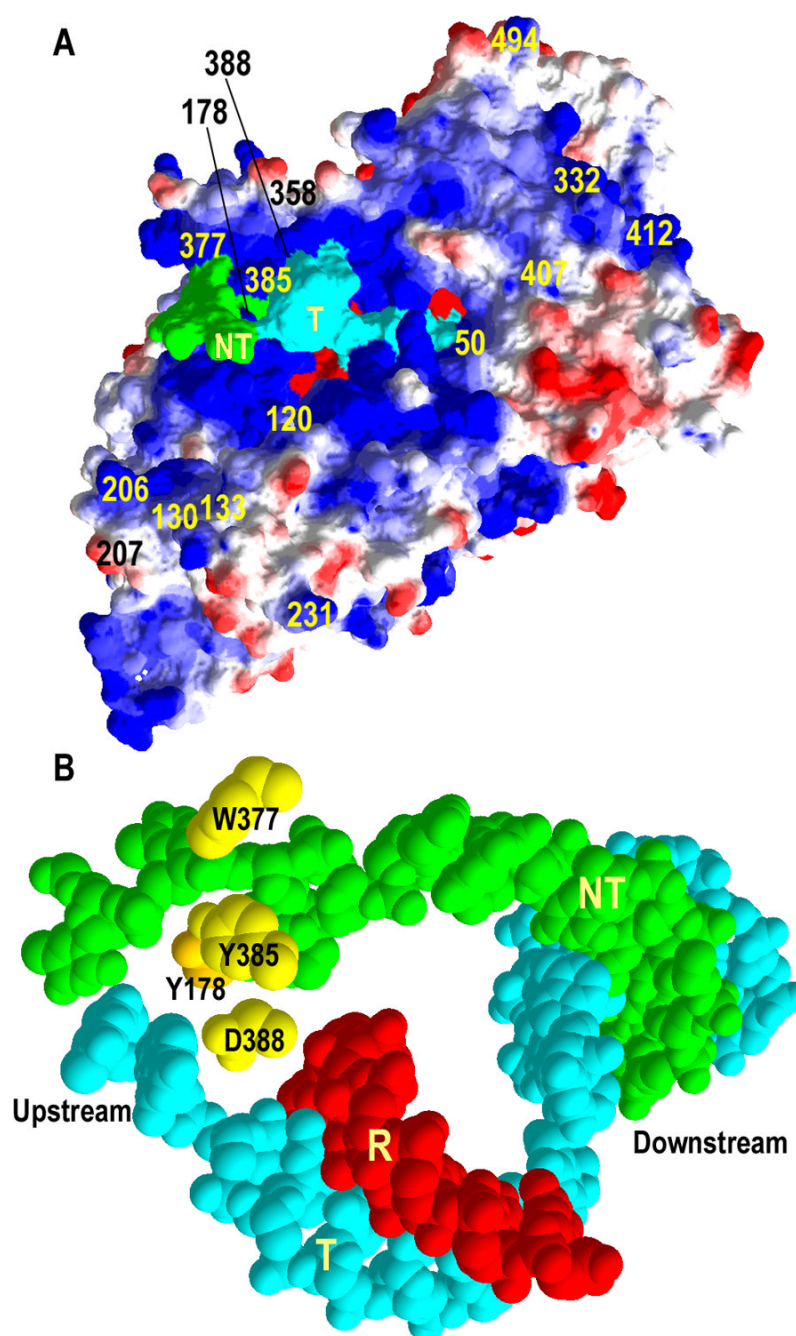


**Figure 2. Residues mutationally scanned for effects on CJ termination**

A: Surface representation of the upstream face of the crystal structure of a T7RNAP EC (pdb 1MSW<sup>24</sup>) with positively charged regions on the polymerase in blue, negatively charged regions in red, the template (T) strand in cyan and the non-template (NT) strand in green. Positions mutated to test effects on CJ termination are indicated by residue number. B: Space-filling representation of nucleic acid structure from the T7RNAP EC with RNA (R) in red and T and NT strands colored as in A. Mutated residues at the upstream edge of the transcription bubble are shown in yellow.

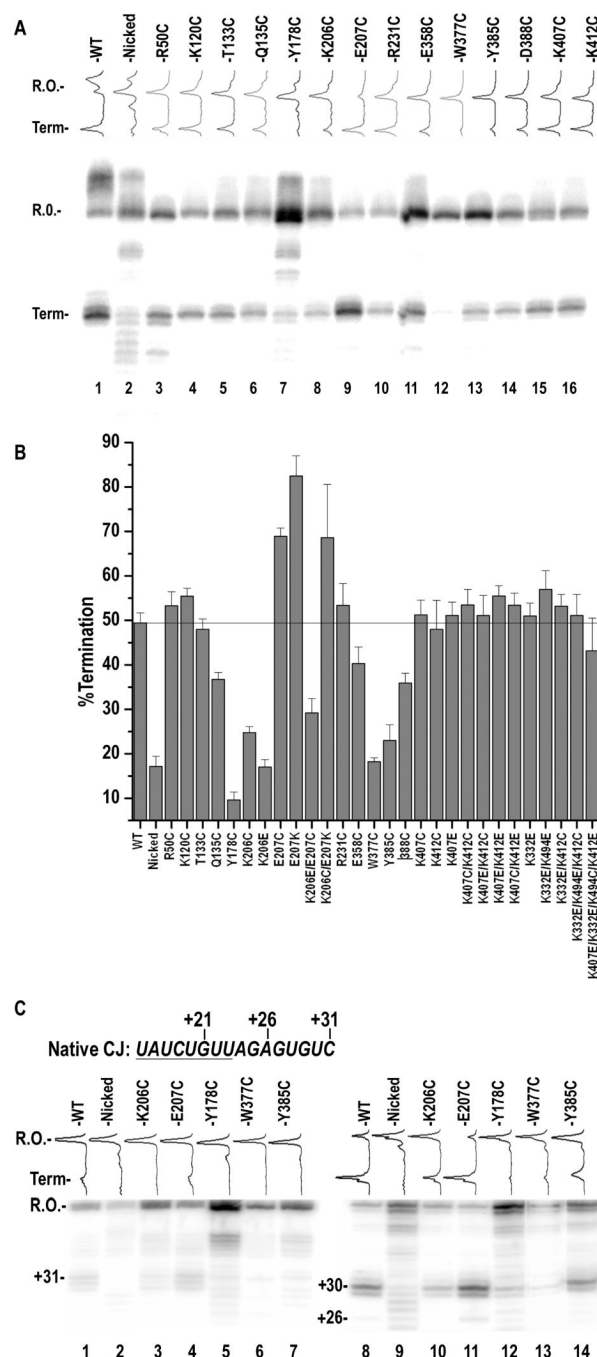


**Figure 3. Effects of RNAP mutations on termination at the CJ**

A: Denaturing page of transcription reactions run with the indicated mutants on *HTSCG66* ('Nicked' in lane 1 refers to an RNAP proteolytically nicked between residues 172 and 173 and which shows reduced termination at the CJ<sup>8</sup>). Scans of each gel lane are shown above the gel image. B: Plot of % termination for the full set of mutants as determined from experiments like those shown in A. Error bars give  $\pm$ s.e. for  $n=3-4$ . C: Termination in either the absence (lanes 1–7) or presence (lanes 8–14) T7 lysozyme on a template (*Native CJ*) in which the sequence downstream of the 8 nt CJ element corresponds to that seen in the T7 genome.

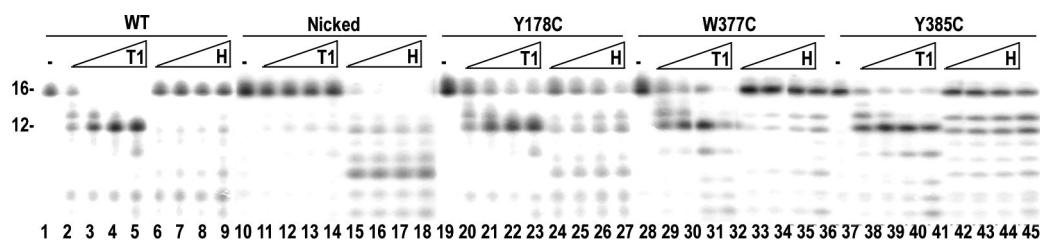


**Figure 4. Mutation of residues at the upstream edge of the transcription bubble reduces RNA displacement activity**

Denaturing PAGE of ECs halted at +15 on *HTSCJ66* and then treated with varying concentrations of RNase T1 or RNase H, as indicated. Lanes 1–9: WT enzyme; lanes 10–18: Nicked enzyme; lanes 19–27: Y178C; lanes 28–36: W377C; lanes 37–45: Y385C.

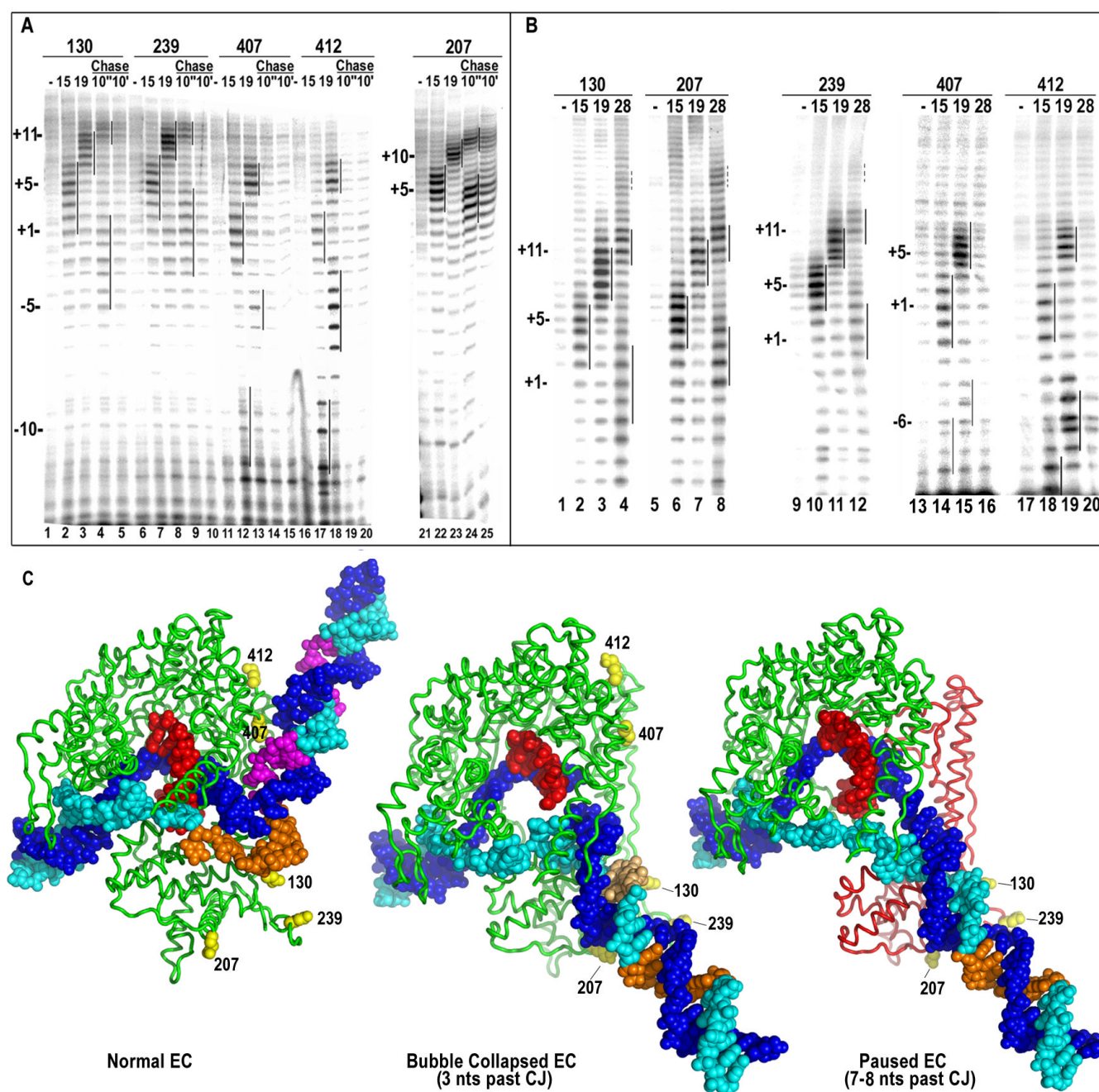


**Figure 5. Changes in tethered chemical nuclease cleavage patterns indicate unbending of upstream DNA and translocational restraint during pausing at the CJ**

**A:** Denaturing PAGE of NT strand cleavage by Fe-BABE conjugated to cysteines introduced at aa 130 (lane 1–5), 239 (lanes 6–10), 407 (lanes 11–15), 412 (lanes 16–20), and 207 (lanes 21–25) in ECs halted at +15 (lanes 2, 7, 12, 17, 22), +19 (lanes 3, 8, 13, 18, 23), or chased for 10 seconds (lanes 4, 9, 14, 19, 24) or 10 minutes (lanes 5, 10, 15, 20, 25) with a complete NTP mix after stopping the EC at +14 by omission of UTP and CTP from the transcription reaction. The template was *HTSCJ66* with the NT strand  $^{32}\text{P}$ -labeled at its 5'-end. Numbering of cleavage positions is relative to the +1 transcription start site. **B:** Experiments as in panel A but with a template (+28 A) in which the U at +28 of *HTSCJ66* has been changed to A. Complexes halted at +28 (lanes 4, 8, 12, 16, 20) were formed by first incubating reactions with

GTP (0.5 mM), ATP (0.01 mM), and UTP (0.1 mM) for 2 min. to form complexes stopped at +18, followed by chasing with 0.5 mM CTP and 0.5 mM 3'-dATP for 5 min. C: Model for structural changes accompanying EC pausing/termination, as inferred from changes in cleavage patterns seen in A and B and previous results that the upstream half of the transcription bubble collapses when the EC transcribes 3 nts past the CJ<sup>20</sup>. "Normal EC": Structure of the T7RNAP EC<sup>23; 24</sup> with the RNAP as a green ribbon and space filling representations of the T- and NT-strands and RNA colored blue, cyan, and red, respectively. Two turns of duplex DNA are modeled upstream of the transcription bubble. Residues to which nucleases were coupled for the experiments in A and B are colored yellow and shown in space-filling representation. Regions on the NT strand that are cut by nucleases at residues 407 and 412 are centered 15 and 25 nts upstream of the RNA 3'-end and are highlighted in *magenta*. Regions cut by nucleases at residues 130, 207, and 239 occur 7–13 nts upstream of the RNA 3'-end and are colored *orange*. "Bubble collapsed EC": Proposed structure of an EC that has transcribed 3 nts past the CJ (corresponding to transcription to +26 on the templates used in panels A and B). The upstream half of the transcription bubble has reannealed, forcing the upstream DNA to unbend. The RNA:DNA hybrid is 3 nts long and the EC is unstable. Cleavage by nucleases at 407/412 is undetectable and the strongest cleavage (highlighted in *orange*) by nucleases at 130/207/239 occurs 13–17 nts upstream of the RNA 3'-end (15–19 nts upstream of the RNA 3'-end in the +28 ECs in panel B). Cleavage by 130/207/239 tracks NT strand accessibility and also occurs ~10 nts upstream of this site (not modeled) and, more weakly, 7–9 nts upstream of the RNA 3'-end (highlighted in *tan*; more downstream regions of the NT strand are protected by the RNAP). "Paused EC": The RNA has been extended 7–8 nts past the CJ and has recovered normal EC hybrid and bubble size<sup>20</sup>. However, the interaction established between the RNAP and the upstream DNA restrains EC translocation so that extension of the RNA is accommodated via scrunching and/or conformational adjustment in the polymerase (suggested in the figure is movement of the red colored N-terminal domain). A limit to these conformational accommodations is reached at this point causing the EC to pause, following which it may release the upstream DNA interaction, recover a normal EC structure and continue elongation, or the strain in the complex may lead to EC dissociation and termination, with the latter favored by a U-rich hybrid<sup>9</sup>.



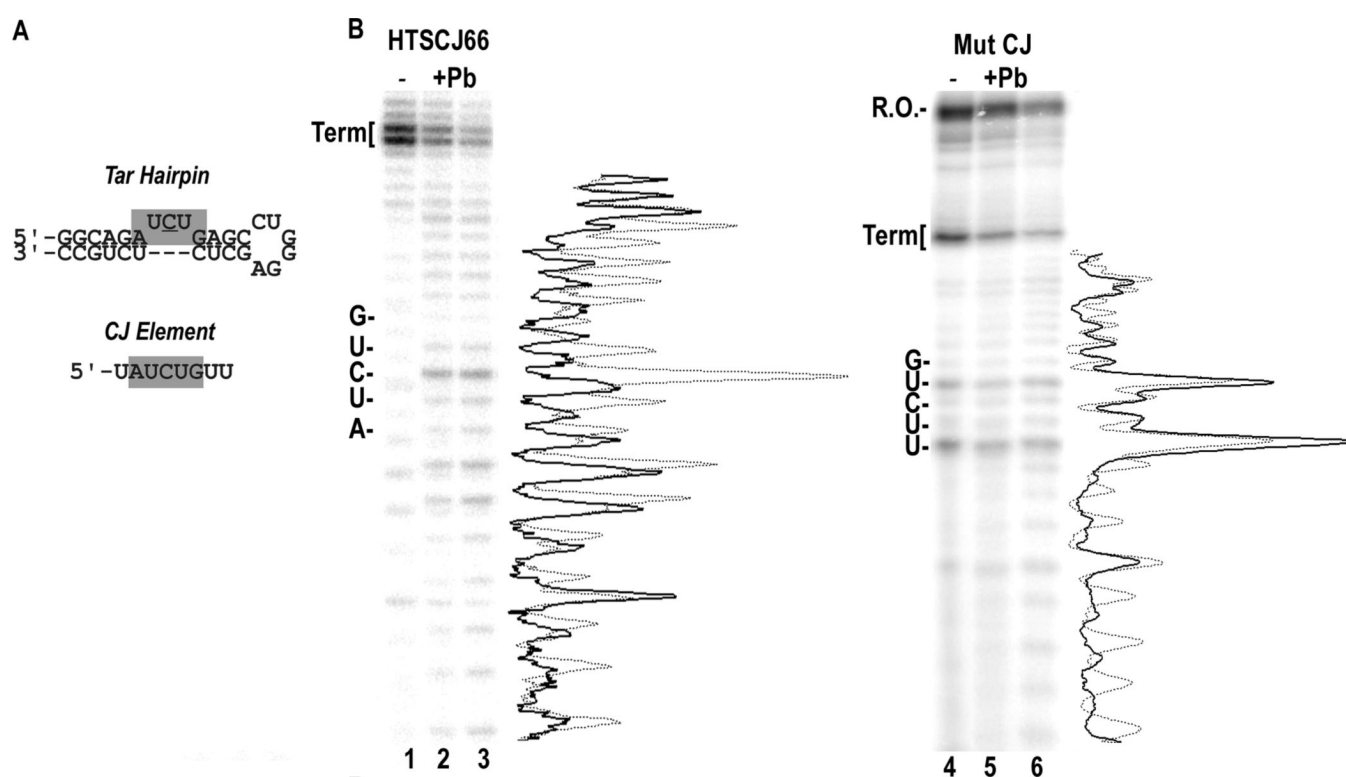


**Figure 6. CJ RNA is specifically cleaved by  $Pb^{++}$  at the same nt at which Tar RNA is cleaved**  
 A: Secondary structure and sequence of the Tar-RNA hairpin and the CJ element. The C that is strongly cleaved by  $Pb^{++}$  in Tar-RNA<sup>30</sup> is underlined. B: Denaturing page of isolated transcripts from reactions run on either *HTSCJ66* (lanes 1–3) or an identical template in which the 1st A of the CJ has been changed to U (*Mut CJ*; lanes 4–6). Transcripts in lanes 2, 5, and 3, 6 were treated with 1mM  $Pb^{++}$  for, respectively, 30 min or 1 hr resulting in low levels of cleavage of the phosphate backbone at all positions and strong cleavage at the central C of the WT CJ element. Scans of the +9 to +29 regions of gel lanes 1, 4 (no Pb) and 3, 6 (+Pb) are shown next to their corresponding gel images with the +Pb scans in dashed lines.

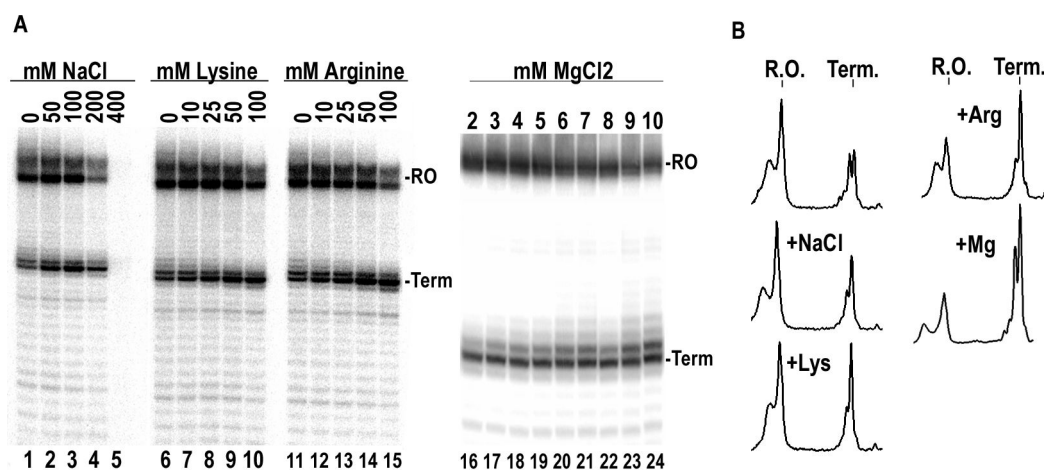


**Figure 7. Arginine and Mg<sup>++</sup> enhance termination at the CJ**

A: Denaturing PAGE of transcription reactions run on *HTSCJ66* in the presence of the indicated concentrations of NaCl (lanes 1–5), lysine (lanes 6–10), arginine (lanes 11–15), or MgCl<sub>2</sub> (lanes 16–24). B: Scans of the following lanes from panel A: no added solute (lane 6); +50 mM NaCl (lane 2); +50 mM lysine (lane 9); +50 mM arginine (lane 14), +10 mM MgCl<sub>2</sub> (lane 24).